Chemical Geology 599 (2022) 120843

Contents lists available at ScienceDirect

Chemical Geology

journal homepage: www.elsevier.com/locate/chemgeo

Thallium isotope compositions of subduction-zone fluids: Insights from ultra-high pressure eclogites and veins in the Dabie terrane, eastern China

Yunchao Shu [a,b,c,*], Sune G. Nielsen [b,d,*], Veronique Le Roux [d], Jerzy Blusztajn [b], Shun Guo [e], Fang Huang [a,f]

[a] CAS Key Laboratory of Crust-Mantle Materials and Environments, School of Earth and Space Sciences, University of Science and Technology of China, Hefei 230026, China
[b] NIRVANA (Non-traditional Isotope Research for Various Advanced Novel Applications) Laboratories, Woods Hole Oceanographic Institution, Woods Hole, MA 02543, USA
[c] The Pheasant Memorial Laboratory for Geochemistry and Cosmochemistry, Institute for Planetary Materials, Okayama University, Misasa, Tottori 682-0193, Japan
[d] Department of Geology and Geophysics, Woods Hole Oceanographic Institution, Woods Hole, MA 02543, USA
[e] State Key Laboratory of Lithospheric Evolution, Institute of Geology and Geophysics, Chinese Academy of Sciences, Beijing 100029, China
[f] CAS Center for Excellence in Comparative Planetology, University of Science and Technology of China, Hefei, Anhui 230026, China

ARTICLE INFO

Editor: Catherine Chauvel

Keywords:
Thallium isotopes
Eclogites
Metamorphic vein
Phengite
Subduction-zone fluids
Dabie orogen

ABSTRACT

Dehydration of the subducted slab is a crucial process in the generation of arc magmas. However, the mineralogical controls of slab dehydration remain uncertain. Thallium (Tl) isotopes have emerged as tracers of subducted slab components, but the Tl isotope characteristics of slab fluids are not known. High-pressure metamorphic veins and host eclogites in the Dabie terrane (China) provide important information on the composition and evolution of subduction zone fluids. In this study, we present the first Tl concentration and Tl isotope data for two high-pressure metamorphic epidote-rich veins formed through breakdown of lawsonite, as well as host eclogites and phengite separates, from the Ganghe and Hualiangting areas. The high Tl concentrations in phengite separates and identical Tl isotope compositions between phengites and their host bulk eclogites demonstrate that phengite controls the overall inventory of Tl in the host eclogites. Generally, the vein samples from both areas have much lower Tl concentrations than their host eclogites, suggesting that the fluids from which the veins precipitated were derived from phengite-bearing eclogites that retained Tl in the residue. The Ganghe eclogites display similar Tl isotope compositions compared with Ganghe omphacite-epidote vein. This similarity indicates that the vein-forming fluid was likely derived from the host eclogites, and that Tl isotopes did not fractionate during fluid-release. Three generations of veins in the Hualiangting area record variable Tl isotope values and were likely derived from multi-stage dehydration of heterogeneous host eclogites, some of which may have contained a sediment component. We argue that fluids derived from eclogite dehydration are likely characterized by higher Cs/Tl ratios compared to their host eclogites. Arc magmas that display high Cs/Tl (i.e. >15) that cannot be caused by variations in slab source composition, coupled with relatively low Ba/Th ratios, are likely to directly record the presence of residual phengite at subarc depths.

1. Introduction

Subduction zones are the primary locations of chemical exchange between the surface and the Earth's interior. In particular, fluids generated from metamorphic dehydration of hydrous minerals in subducted slabs are viewed as important agents for the transfer of slab-derived materials into the overlying mantle wedge (Peacock, 1990; Ulmer and Trommsdorff, 1995; Kessel et al., 2005; Harvey et al., 2014; Kendrick et al., 2014; Scambelluri et al., 2015; Keppler, 2017; Villalobos-Orchard et al., 2020). Although such fluids cannot be sampled in-situ, eclogite-facies veins preserved in high-pressure (HP) and ultra-high-pressure (UHP) metamorphic rocks record fluid-rock interactions that occurred at sub-arc depths (Gao and Klemd, 2001; Spandler and Hermann, 2006; Gao et al., 2007; Zhu et al., 2020).

* Corresponding authors at: NIRVANA (Non-traditional Isotope Research for Various Advanced Novel Applications) Laboratories, Woods Hole Oceanographic Institution, Woods Hole, MA 02543, USA.
E-mail addresses: yshu@ustc.edu.cn (Y. Shu), snielsen@whoi.edu (S.G. Nielsen).

https://doi.org/10.1016/j.chemgeo.2022.120843
Received 21 July 2021; Received in revised form 9 March 2022; Accepted 28 March 2022
Available online 31 March 2022
0009-2541/

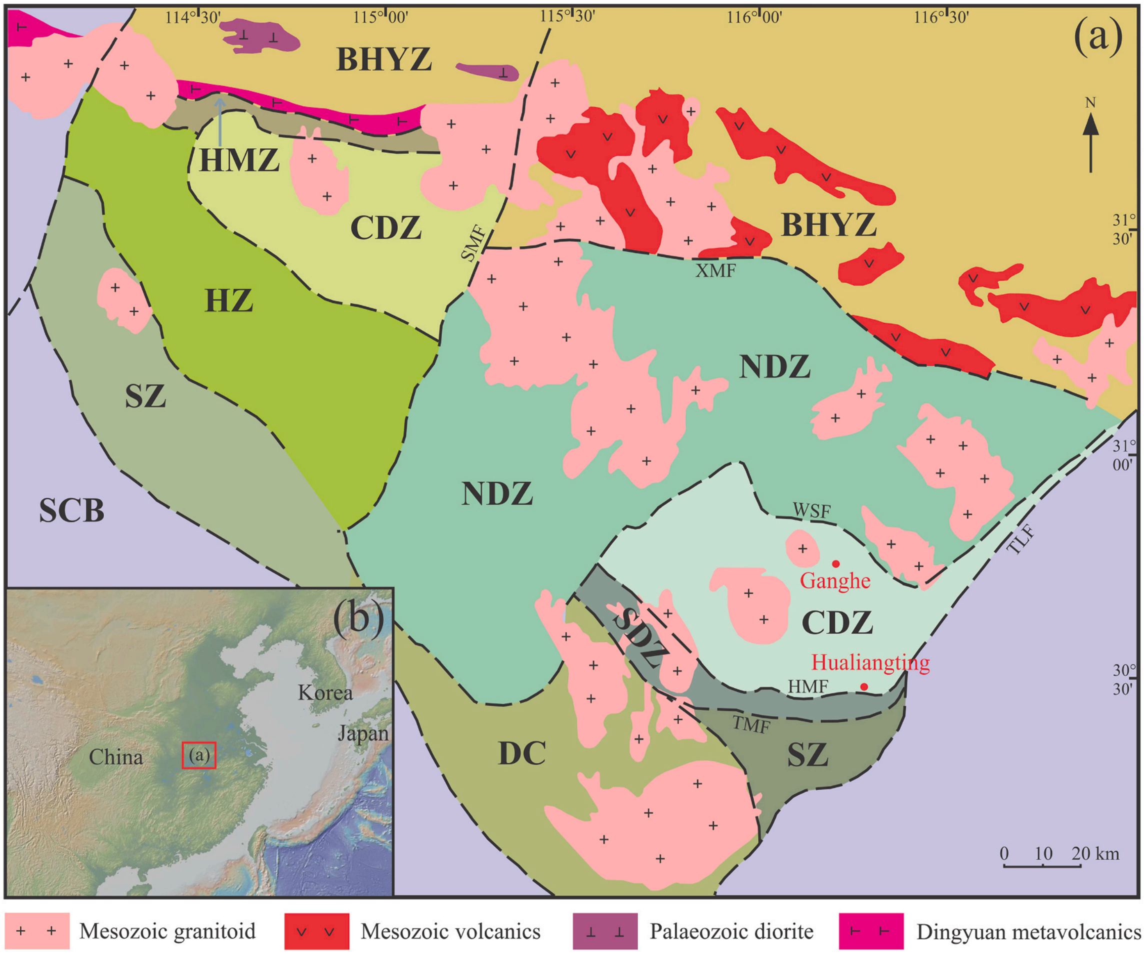

Fig. 1. Sketch map of geology for the Dabie orogeny (modified after (Liu et al., 2007)), with inset showing the location of this area in Asia. Sample localities are shown using red dots. BHYZ, Beihuaiyang zone; NDZ, North Dabie high-temperature and ultra-high pressure complex zone; CDZ, Central Dabie middle-temperature and ultra-high pressure metamorphic zone; SDZ, South Dabie low-temperature eclogite zone; SZ, Susong complex zone; HMZ, Huwan mélange zone; HZ, Hong'an low-temperature eclogite facies zone; DC, amphibolite facies Dabie complex; XMF, Xiaotian-Mozitan fault; WSF, Wuhe-Shuihou fault; HMF, Hualiangting-Mituo fault; TMF, Taihu-Mamiao fault; SMF, Shang-Ma fault; TLF, Tan-Lu fault; SCB, South China block. Dashed lines represent boundaries of different metamorphic zones. (For interpretation of the references to colour in this figure legend, the reader is referred to the web version of this article.)

In this study, we present thallium (Tl) concentrations and Tl isotope compositions of two suites of well-characterized high-pressure metamorphic veins and their host eclogites at Ganghe and Hualiangting in the Dabie orogen, eastern China. Thallium is a highly incompatible, fluid-mobile and lithophile element (Shaw, 1952; Shannon, 1976; Heinrichs et al., 1980; Nielsen et al., 2014; Nielsen et al., 2017) that has two stable isotopes, ^{203}Tl and ^{205}Tl. Its isotope composition is reported in epsilon units relative to the NIST SRM 997 Tl standard in parts per 10,000 ($\varepsilon^{205}\mathrm{Tl} = 10{,}000 \times (^{205}\mathrm{Tl}/^{203}\mathrm{Tl}_{\mathrm{sample}} - {}^{205}\mathrm{Tl}/^{203}\mathrm{Tl}_{\mathrm{SRM997}}) \div {}^{205}\mathrm{Tl}/^{203}\mathrm{Tl}_{\mathrm{SRM997}}$). Pelagic sediments typically record heavy Tl isotope compositions of $\varepsilon^{205}\mathrm{Tl} > +2$ (Prytulak et al., 2013; Nielsen et al., 2016; Nielsen et al., 2017; Shu et al., 2017), because they usually contain significant authigenic manganese oxide components with high Tl concentrations and heavy Tl isotope compositions of up to $\varepsilon^{205}\mathrm{Tl} \sim +15$ (Rehkämper et al., 2002; Rehkämper et al., 2004; Nielsen et al., 2013). The upper altered oceanic crust, on the other hand, exhibits light Tl isotope values of $\varepsilon^{205}\mathrm{Tl} < -2$ (Nielsen et al., 2006c; Coggon et al., 2014; Shu et al., 2017) due to incorporation of seawater-derived Tl which in modern open ocean is characterized by $\varepsilon^{205}\mathrm{Tl} = -6$ (Owens et al., 2017). In contrast, the depleted mid-ocean ridge mantle (DMM) displays homogeneous Tl isotope compositions of $\varepsilon^{205}\mathrm{Tl} \sim -2$ (Nielsen et al., 2006b; Nielsen et al., 2006c). Therefore, the Tl isotope system has successfully been used to trace recycling of crustal materials in arc magmas and ocean island basalts (OIBs) due to the distinctive Tl isotope compositions of subducted slab components compared with upper mantle (Nielsen et al., 2006b; Nielsen et al., 2007; Prytulak et al., 2013; Nielsen et al., 2015; Nielsen et al., 2016; Nielsen et al., 2017; Shu et al., 2017; Blusztajn et al., 2018; Brett et al., 2021; Williamson et al., 2021). However, studies on the Tl isotope compositions of subduction-zone fluids and the behavior of Tl isotopes during fluid-rock interaction at subarc depths remain limited (Shu et al., 2019). Here, we provide new information on the elemental and isotope variations of Tl during dehydration of eclogites and demonstrate how the Cs/Tl ratios of eclogite-derived fluids can be controlled by the presence of phengite in subducted slabs.

2. Geological setting

The samples consist of UHP eclogites and HP metamorphic veins that were collected from the Ganghe and Hualiangting areas, located in the central Dabie UHP metamorphic zone (Fig. 1). The HP metamorphic veins and their host UHP eclogites have been geochemically and petrologically characterized in previous studies (Guo et al., 2012; Guo et al., 2014; Guo et al., 2015a). These metamorphic rocks formed from continental basalts that represent remnants of a subducted (at depths of >100 km) and exhumed continental slab (Li et al., 1993; Zheng et al., 2003; Zhang et al., 2009; Zheng et al., 2009). The Dabie UHP metamorphic terrane is the western part of the Dabie-Sulu orogenic belt in

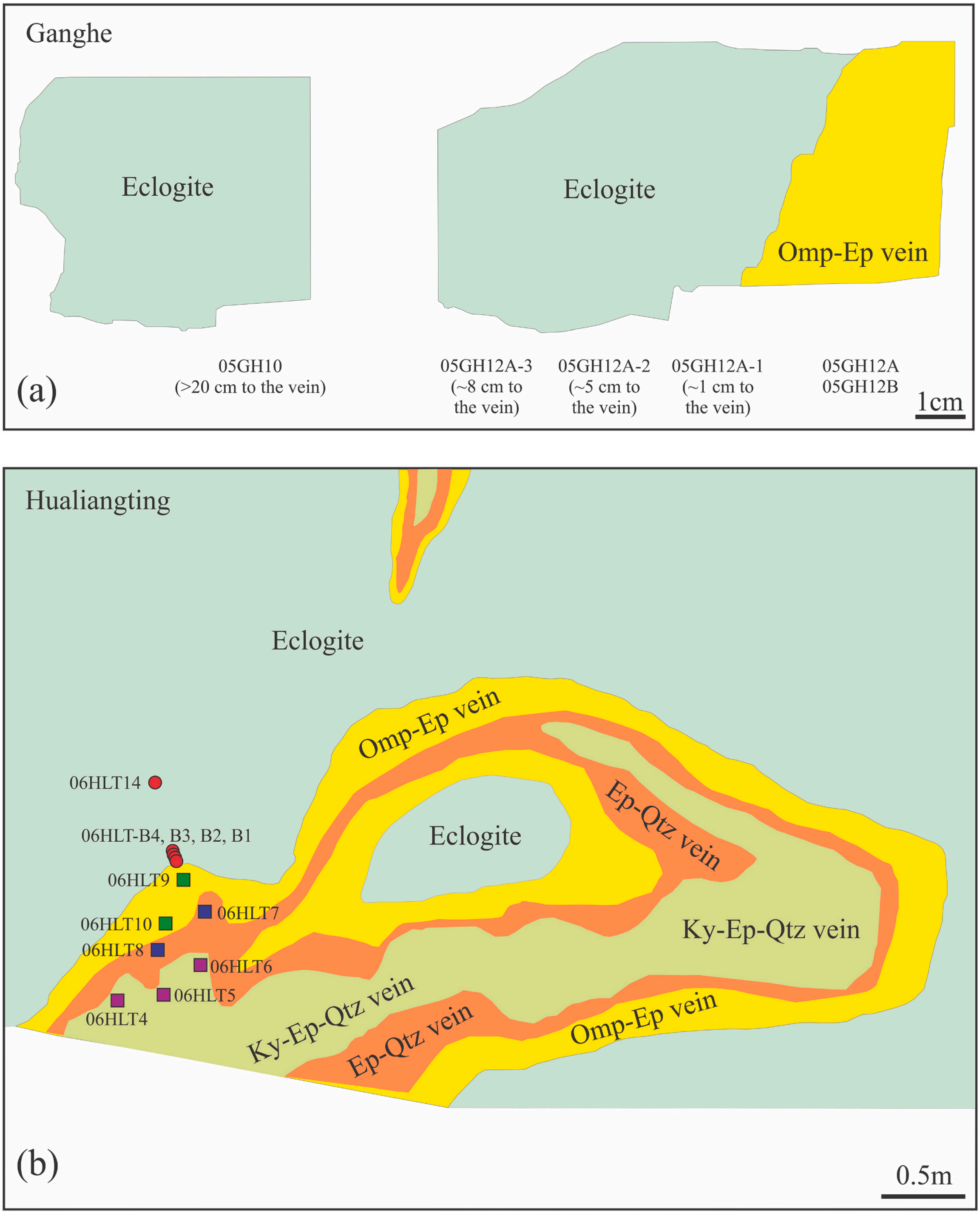

Fig. 2. Schematic maps illustrating the relationships of the eclogites and veins in (a) Ganghe (modified after photograph of polished hand samples (Guo et al., 2012)) and (b) Hualiangting (modified after (Guo et al., 2015a)). Sample locations are also shown on the maps. Field photographs were provided in Supplementary Information. Omp, omphacite; Ep, epidote; Qz, quartz; Ky, kyanite. The colors used for the sample symbols are the same in Figs. 3–5 and 7.

eastern China. It formed by continental subduction of the Yangtze Craton beneath the Sino-Korean lithospheric plate between ~240 and ~220 Ma and is one of the largest exposed UHP metamorphic terrane on Earth (Li, 1993; Zheng et al., 2003; Zheng et al., 2006a; Zhang et al., 2009; Zhao et al., 2018). From north to south, the Dabie terrane is divided into (1) a low-grade metamorphic belt (Beihuaiyang zone), (2) the north Dabie high-T/P amphibolite/granulite belt, (3) the central Dabie UHP belt from where our samples were collected, (4) a narrow coesite-free eclogite belt and (5) an epidote amphibolite + narrow blueschist belt (Susong complex zone) (Zhang et al., 1996). Eclogite rocks are widespread in the Dabie terrane as lenses, layers or blocks in gneiss, peridotite and marble and characterized by common occurrences of coesite and/or quartz pseudomorphs after coesite as inclusion in garnet, omphacite and zircon (Zhang et al., 2009). The diamonds and diamondiferous rocks including eclogite, garnet-pyroxenite and jadeitite in central Dabie UHP belt are interpreted to be the products of UHP metamorphism at greater than 4.0 GPa and 900 °C (Xu et al., 1992). The veins in Dabie terrane are considered to have formed through initial eclogitic conditions of 1.8–2.3 GPa and 500–600 °C triggered by prograde dehydration of lawsonite during subduction (Castelli et al., 1998;

Table 1
Modal abundance of major and minor phases in vol% for Ganghe and Hualiangting UHP eclogites and veins.[a]

Sample	Location	Rock types	Grt	Omp	Ep	Qz	Ky	Amp	Ph	Accessory mineral (Rt, Zrn, Ap)
Ganghe	30°41′53"N, 116°14′82″E									
05GH10		Eclogite (~20 cm to the vein)	25	27	21	7	6	7	3	4
05GH12A-3		Eclogite (~8 cm to the vein)	30	37	16			8	4	5
05GH12A-2		Eclogite (~4.75 cm to the vein)	32	38	7			7	10	6
05GH12A-1		Eclogite (~1.25 cm to the vein)	40	40				10	2	8
05GH12A		Omp-Ep vein	<5	30	50	5		5	<1	5
05GH12B		Omp-Ep vein	<5	30	50	5		5	<1	5
Hualiangting	30°28′17.3"N, 116°15′03.2″E									
06HLT14		Eclogite (~50 cm to the vein)	30	25	20	7	7	4	1	6
06HLT-B4		Eclogite (~7 cm to the vein)	35	28	14	4	5	4	5	5
06HLT-B3		Eclogite (~5 cm to the vein)	38	30	7		2	8	9	6
06HLT-B2		Eclogite (~3 cm to the vein)	40	36	5			8	5	6
06HLT-B1		Eclogite (~1 cm to the vein)	44	42				4	2	8
06HLT9		Omp-Ep vein		22	60	9		4		5
06HLT10		Omp-Ep vein		15	65	10		5		5
06HLT7		Ep-Qz vein		5	45	40		5	<1	5
06HLT8		Ep-Qz vein		5	47	38		5	<1	5
06HLT4		Ky-Ep-Qz vein		4	16	62	10	1	2	5
06HLT5		Ky-Ep-Qz vein		4	14	64	10	1	2	5
06HLT6		Ky-Ep-Qz vein		3	12	68	8	1	3	5

Grt-garnet; Omp-omphacite; Ep-epidote; Qz-quartz; Ky-kyanite; Amp-amphibole; pH-phengite; Rt-rutile; Zrn-zircon; Ap-apatite.
[a] Mineral assemblages and mineral volume abundances are from (Guo et al., 2012; Guo et al., 2014; Guo et al., 2015a). The modal (quantitative mineralogical) analysis of samples is generally determined by point-counting method on thin sections.

Franz et al., 2001). The protolith ages of eclogite and gneiss are Paleoproterozoic to Neoproterozoic (1820–680 Ma), but most are Neoproterozoic (~750 Ma) (Zheng et al., 2006b).

2.1. Ganghe eclogite and vein samples

The Ganghe samples (30°41′53"N, 116°14′82″E) were collected from a roadside outcrop near the Ganghe village in Yuexi County, which is located within the coesite-eclogite-facies metamorphic zone (Fig. 1). The Ganghe massive eclogite experienced UHP metamorphism, with peak P-T conditions of about 3.1 GPa and 650 °C, and eclogite-facies and amphibolite-facies retrogression at about 1.5 GPa and 600 °C and < 1.1 GPa and < 600 °C respectively (Guo et al., 2015b). The Ganghe massive eclogites contain yellow-green colored veins that are less than one to several centimeters in width and several centimeters to a few meters in length and usually crosscut the eclogite (Guo et al., 2012). A series of three eclogite samples with a diameter of ~2 cm each were collected along a profile line perpendicular to the vein: 05GH12A-3 (7–9 cm to the vein), 05GH12A-2 (~4.75 cm to the vein) and 05GH12A-1 (0–2.5 cm to the vein) (Fig. 2a and Table 1). For comparison, an eclogite collected further away from the vein (05GH10, ~20 cm to the vein) represents the unmodified distal sample. Finally, two omphacite-epidote vein samples were also sampled (05GH12A and 05GH12B). These samples include eclogite and vein that have been characterized for major and trace elements as well as other stable isotope compositions in previous studies (Guo et al., 2012; Huang et al., 2020; Li et al., 2020). Here we only briefly summarize them. The main minerals in all eclogites are omphacite and garnet (Table 1), similar to eclogites found in oceanic settings. The most prominent change in the matrix of eclogite toward the vein is characterized by the systematic decrease of porphyroblastic kyanite, quartz and epidote and increase of proportions of fine-grained garnet, omphacite and rutile. The mineral assemblage, mineral abundance, grain shape and grain size of kyanite, quartz and epidote in the eclogites (from 05GH12A-3 to 05GH12A-1, Fig. 2a) change gradually toward the vein. These features demonstrate that significant fluid-eclogite interaction took place during fluid release and mineral dissolution-precipitation led to remarkable mass transfer from host UHP eclogite to HP vein (Guo et al., 2012). The late-stage amphibole and phengite porphyroblasts occur in all eclogites (Table 1). The metamorphic veins are mainly composed of epidote and omphacite with minor garnet, quartz, apatite, rutile and zircon (hereafter referred to omphacite-epidote vein). They are enclosed in the interior of the host eclogites and never observed in the country-rock gneisses (Guo et al., 2012). Observations of lawsonite pseudomorphs, combined with phase equilibrium modeling, indicate that the vein-forming fluid was produced by the breakdown of lawsonite at pressures of 2.8–3.0 GPa and temperatures lower than 680 °C (Guo et al., 2012). The omphacite-epidote vein has a sharp boundary with the host eclogite (Fig. S2b). The proportions of amphibole and phengite in the vein are significantly lower or absent compared with host eclogite (Guo et al., 2012). The omphacite-epidote vein suffered very weak retrogression metamorphism. In order to ascertain the influence of retrogression, the weakly retrograde omphacite-epidote vein (sample 05GH12B) will be compared with pristine sample 05GH12A. The two samples have a similar mineral assemblage, except for small amounts of late-stage disseminated amphibolite-facies veinlets that crosscut the matrix minerals (Table 1) in sample 05GH12B (Guo et al., 2014). Representative micrographs pictures of the samples are presented in Supplementary Information and Guo et al. (2012, 2014 and 2015b).

2.2. Hualiangting eclogite and vein samples

The Hualiangting area (30°28′17.3"N, 116°15′03.2″E) is located near the boundary between central Dabie UHP metamorphic zone and south Dabie low-T eclogite zone (Fig. 1). The Hualiangting eclogite originated from a granulite precursor along an anticlockwise *P-T* path and the estimated peak *P-T* conditions are greater than 3.5 GPa and 800 °C (Massonne, 2012). A successive profile of four eclogite samples, with a diameter of approximately 2 cm each along a line perpendicular to the eclogite-vein contact (6–8 cm for 06HLT-B4, 4–6 cm for 06HLT-B3, 2–4 cm for 06HLT-B2, and 0–2 cm for 06HLT-B1), were sampled to evaluate the chemical effect of the fluid-rock interaction (Fig. 2b and Table 1). For comparison, an eclogite collected further away from the vein (06HLT14, ~50 cm to the vein) represents the unmodified distal sample. In addition, two omphacite-epidote veins (06HLT9 and 06HLT10), two epidote-quartz veins (06HLT7 and 06HLT8) and three kyanite-epidote-quartz veins (06HLT4, 06HLT5 and 06HLT6) were collected (Fig. 2b and Table 1). These eclogites and veins have been characterized in previous studies (Guo et al., 2015a; Huang et al., 2020; Li et al., 2020), so we only briefly summarize them here. The eclogite consists of garnet, omphacite, epidote, kyanite, quartz and amphibole, with minor amounts of talc, phengite and accessory apatite, rutile and

Table 2
Thallium concentration and isotope compositions together with selected major and trace elements of Ganghe and Hualiangting UHP eclogites and veins.

Sample	K_2O (wt%)	Cs (μg/g)	Cu (μg/g)	Rb (μg/g)	Ba (μg/g)	Tl (ng/g)	2sd[a]	Cs/Tl	2sd	$^{87}Sr/^{86}Sr$	$\delta^{138/134}Ba$	$\varepsilon^{205}Tl$	2sd[b]	n[c]
Ganghe														
Eclogite														
05GH10	0.68	0.77	14.0	21.9	307	95.5	14.3	8.02	1.20	0.70710	0.03	−1.2	0.4	2
Phengite						1342	201					−1.5	0.4	2
05GH12A-3	0.99	1.46	15.7	33.7	416	218	33	6.70	1.00	0.70703	0.03	−0.8	0.4	2
05GH12A-2	1.51	2.11	12.1	54.5	653	101	15	20.9	3.1	0.70711	0.03	−1.1	0.4	2
Phengite						1271	191					−1.2	0.4	2
05GH12A-1	0.61	0.63	13.6	19.3	247	104	16	6.06	0.91	0.70701	−0.01	−1.2	0.4	2
Omp-Ep vein														
05GH12A	0.02	0.05	9.65	1.39	56.7	2.82	0.42	17.0	2.6	0.70708	0.17	−1.1	0.4	2
Replicate						3.01	0.45					−1.0	0.4	2
05GH12B						5.23	0.78					−1.1	0.4	2
Hualiangting														
Eclogite														
06HLT14	0.03	0.06	35.0	0.93	38.0	3.39	0.51	17.7	2.7	0.70440	0.03	−2.8	0.4	2
06HLT-B4	0.59	0.67	43.6	11.1	533	28.4	4.3	23.6	3.5	0.70431	−0.14	−1.9	0.4	2
Phengite						438	66					−1.7	0.4	2
06HLT-B3	0.73	1.17	43.6	13.6	684	26.2	3.9	44.7	6.7		−0.10	−1.9	0.4	2
06HLT-B2	0.51	0.54	59.1	8.56	493	5.64	0.85	95.7	14.4	0.70432	−0.08	−1.7	0.4	2
06HLT-B1	0.17	0.62	34.8	9.82	577	35.6	5.3	17.4	2.6	0.70429	0.05	−1.9	0.4	2
Omp-Ep vein														
06HLT9	0.04	0.02	28.5	0.40	110	1.04	0.16	19.2	2.9	0.70440	−0.17	−0.9	0.4	2
06HLT10	0.02	0.05	35.5	0.42	167	1.47	0.22	34.0	5.1		0.17	+1.6	0.4	2
Ep-Qz vein														
06HLT7		0.05	6.21	0.81	58.8	0.67	0.10	74.6	11.2	0.70439	−0.11	+1.1	0.4	2
Replicate						0.59	0.09					+1.3	0.4	2
06HLT8	0.01	0.05	5.31	0.68	50.4	0.54	0.08	92.6	13.9		0.34	+1.1	0.4	2
Ky-Ep-Qz vein														
06HLT4		0.09	13.2	1.38	35.4	1.98	0.30	45.5	6.8		0.15	−2.2	0.4	2
06HLT5	0.07	0.16	10.1	2.17	66.5	1.48	0.22	108	16	0.70434	0.12	−2.3	0.4	2
06HLT6	0.07	0.17	11.2	2.20	30.9	1.87	0.28	90.9	13.6		0.14	−2.5	0.4	2

Omp-omphacite; Ep-epidote; Qz-quartz; Ky-kyanite.
K_2O, Cs, Cu, Rb and Ba contents and whole-rock $^{87}Sr/^{86}Sr$ ratios from (Guo et al., 2012; Guo et al., 2014; Guo et al., 2015a), Ba isotope data from (Gu et al., 2021). Both the precision and accuracy of the whole-rock major and trace elements are generally better than 5%, as shown by the analyses of three international rock reference materials GSR-1, GSR-2 and GSR-3 and duplicate analyses of a particular sample (06HLT-B4) (Guo et al., 2012; Guo et al., 2015a).
[a] The long-term reproducibility of Tl concentrations in silicate samples is ±15% (2sd).
[b] We analyzed two times each sample using mass spectrometry for Tl isotope data. Although individual Tl isotope analyses have uncertainties of 0.02–0.28 (2sd), we apply the external 2sd reproducibility of 0.4 ε^{205}Tl-units to all unknowns because this uncertainty accounts for all possible sources of error including sample dissolution, ion exchange chromatography and mass spectrometric procedures.
[c] n represents the numbers of mass spectrometry analyses for the same sample.

zircon. Like the Ganghe samples, mineral abundances and grain sizes of epidote, kyanite and quartz porphyroblasts in the eclogites continuously decrease toward the vein interpreted as a result of fluid-eclogite interaction (Guo et al., 2015a). The abundances of garnet and omphacite in the eclogites gradually increase as the vein is approached. The Hualiangting UHP massive eclogites contain abundant HP veins with large variations in the mineral assemblages at different spatial locations. Petrologic observations (e.g. existence of lawsonite pseudomorphs) and chemical analyses indicate that the vein-forming fluids were primarily produced by the breakdown of lawsonite in the host eclogites at *P-T* conditions of 2.7–3.0 GPa and 660–720 °C (Guo et al., 2015a). The interfaces between the veins and eclogites are typically sharp. From the vein-eclogite boundary to the vein interior, three types of veins can be observed: omphacite-epidote veins, epidote-quartz veins and kyanite-epidote-quartz veins. Phengite was rarely observed in these veins (Guo et al., 2015a). Photograph and micrographs of the eclogite and vein samples are available in Supplementary Information and Guo et al. (2015a).

3. Methods

3.1. Sample preparation

We used aliquots of the same powders for eclogites and veins that were previously investigated for major and trace elements and other isotope systems (Guo et al., 2012; Guo et al., 2015a; Huang et al., 2020; Li et al., 2020). Optically clean phengite mineral grains were handpicked under binocular microscope, then cleaned three times with ethanol in an ultrasonic bath for 10 min. Powdered eclogite and vein samples of 0.1–0.3 g and phengite minerals of 0.01–0.04 g were digested in a 1:5 mixture of concentrated distilled HF and HNO_3 on a hotplate for 24 h. They were then dried and fluxed several times using a 1:1 mixture of concentrated distilled HNO_3 and HCl until the fluorides that formed in the first step were completely dissolved. Some samples that did not completely dissolved using above steps were dried on a hotplate and dissolved in concentrated distilled HNO_3, then digested using a high-pressure asher at pressure and temperature up to 10 MPa (100 bar) and 260 °C. Following complete dissolution of fluorides, all samples were dried again on a hotplate and dissolved in 1 M hydrochloric acid for ion exchange chromatographic separation of Tl. Thallium was separated from the matrix of samples in the NIRVANA (Non-traditional Isotope Research for Various Advanced Novel Applications) clean lab at Woods Hole Oceanographic Institution (WHOI). Isolation of Tl from sample matrix followed previously published ion exchange chromatographic methods (Rehkämper and Halliday, 1999; Nielsen et al., 2004). Total procedural blanks including sample dissolution and column chemistry for Tl were determined for every set of samples processed through the column chemistry and were always <2 pg, which is significantly less than the minimum amounts of Tl processed (>1 ng), therefore, negligible.

3.2. Measurement of thallium concentration and isotope compositions

The thallium isotope compositions were analyzed on a Thermo

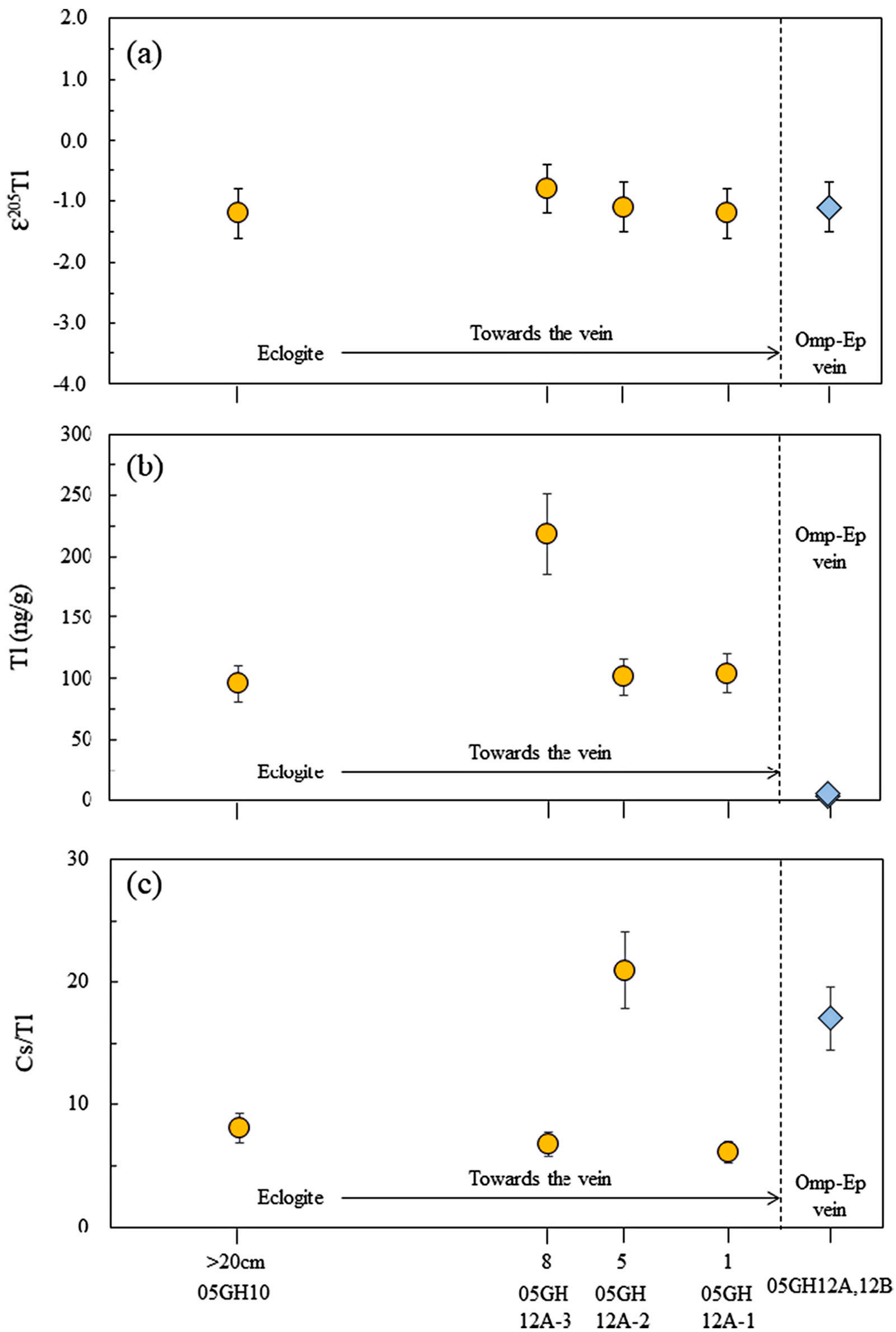

Fig. 3. Variation of (a) thallium isotope compositions, (b) thallium concentrations and (c) Cs/Tl ratios of the eclogite and vein samples at Ganghe. Numbers in the x-axis show the average distances (cm) from the center of the sample to the eclogite-vein boundary. The error bars for Tl isotopes and concentrations in this and following figures represent the long-term reproducibility of Tl isotopes and concentrations in silicate samples of ±0.4 ε^{205}Tl-units (2sd) and ± 15% (2sd) respectively.

Finnigan Neptune multicollector inductively coupled plasma mass spectrometer (MC-ICP-MS), located in the Plasma Facility at the Woods Hole Oceanographic Institution. External correction for mass discrimination to NIST SRM 981 Pb and standard sample bracketing of the NIST SRM 997 Tl standard were applied for analysis of Tl isotope compositions (Rehkämper and Halliday, 1999; Nielsen et al., 2004). The Tl separation procedure has been shown to produce quantitative yields (Nielsen et al., 2004; Rehkämper et al., 2004; Nielsen et al., 2006a). Thus, thallium concentrations were determined by monitoring the ^{205}Tl intensity during the isotope measurements relative to the known quantity of NIST SRM 981 Pb added to perform external mass bias corrections. The measured ^{205}Tl/^{208}Pb ratios was converted into a mass of Tl processed and then Tl concentrations were determined by reference to the amount of sample digested. The secondary reference material, USGS basalt powder BHVO-1, was also processed with every set of unknowns and displayed consistent Tl isotope composition of ε^{205}Tl = −3.6 ± 0.4 (2sd, n = 61) and Tl concentration of 39.0 ± 5.7 ng/g (2sd) (Table S1), which is in excellent agreement with previous work (Nielsen

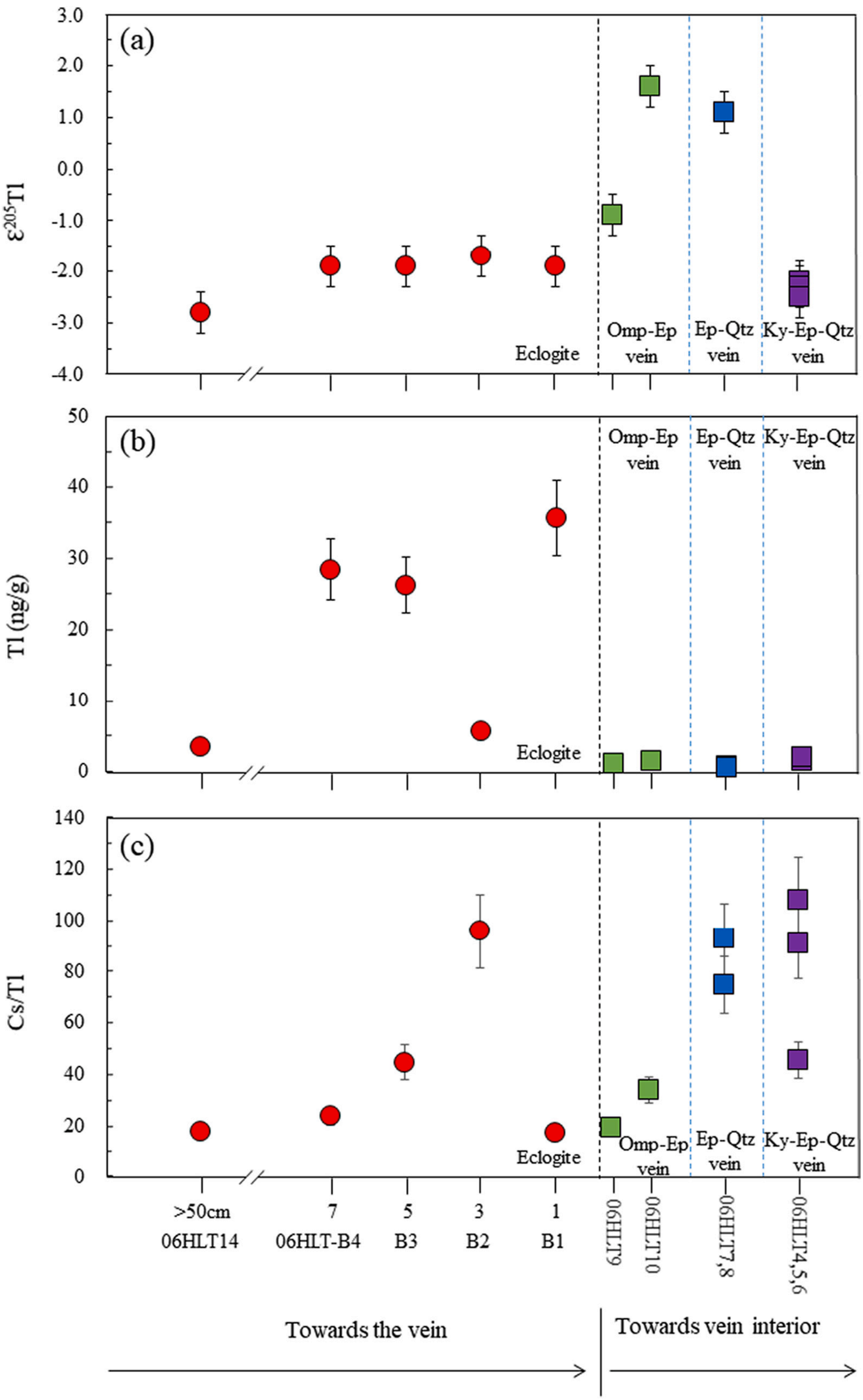

Fig. 4. Variation of (a) thallium isotope compositions, (b) thallium concentrations and (c) Cs/Tl ratios of the eclogites and veins at Hualiangting. Numbers in the x-axis show the average distances (cm) from the center of the sample to the eclogite-vein boundary. The omphacite-epidote vein has a sharp contact with the host eclogites, the kyanite-epidote-quartz vein locates at the inner part of the multiple veins, and epidote-quartz vein lies between omphacite-epidote and kyanite-epidote-quartz veins.

et al., 2015; Nielsen et al., 2016; Shu et al., 2017; Shu et al., 2019). The long-term reproducibility of Tl isotopes and concentrations in silicate samples are ±0.4 ε^{205}Tl-units (2sd) and ± 15% (2sd), respectively. We use these uncertainties throughout this study as our best estimates of the total external error on individual Tl isotope and concentration measurements, because these uncertainties account for all possible sources of error including sample dissolution, ion exchange chromatography and mass spectrometric procedures (Nielsen et al., 2004).

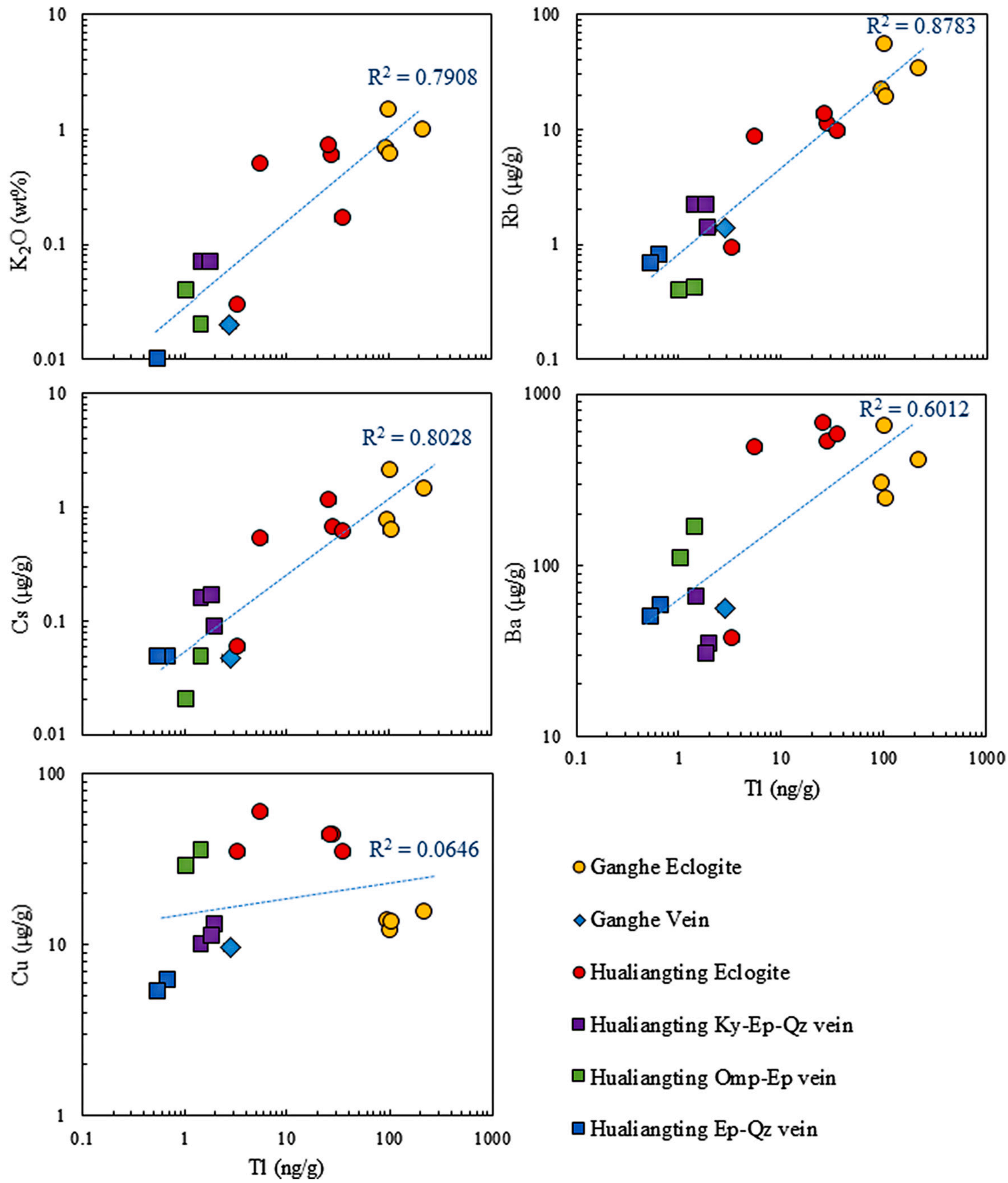

Fig. 5. Thallium concentration (ng/g) plotted against K_2O (wt%), Rb (μg/g), Cs (μg/g), Ba (μg/g) and Cu (μg/g) contents in eclogites and veins from Ganghe and Hualiangting. K_2O, Rb, Cs, Ba and Cu contents are from previous studies (Guo et al., 2012; Guo et al., 2015a).

4. Results

4.1. *Thallium concentration and isotope compositions of vein and host eclogites from Ganghe*

Ganghe metamorphic omphacite-epidote vein samples 05GH12A displays ε^{205}Tl = −1.1 and Tl concentrations of 2.82 ng/g (Table 2). The weakly retrograde omphacite-epidote vein sample 05GH12B has identical Tl isotope composition of ε^{205}Tl = −1.1 and similar low Tl concentration (5.23 ng/g) compared to sample 05GH12A. Ganghe eclogites far from the vein (05GH10) and near the vein (05GH12A-1, 05GH12A-2 and 05GH12A-3) exhibit ε^{205}Tl values from −0.8 to −1.2 (Table 2), which is indistinguishable from Ganghe omphacite-epidote veins (Fig. 3). Thallium concentrations in the distal eclogite (95.5 ng/g) and in those close to the vein (101 to 218 ng/g) are relatively similar (Table 2).

4.2. *Thallium concentration and thallium isotope variations of veins and host eclogites from Hualiangting*

The eclogite 06HLT14 far from the vein displays a Tl isotope value of ε^{205}Tl = −2.8, which is slightly lighter than those of the eclogites near the vein (06HLT-B1, 06HLT-B2, 06HLT-B3 and 06HLT-B4; ε^{205}Tl = −1.7 to −1.9) (Table 2). Compared to the distal host eclogites, omphacite-epidote vein samples (06HLT9 and 06HLT10) located near the vein-eclogite boundary have heavier Tl isotope compositions of ε^{205}Tl = −0.9 and + 1.6 (Table 2). Two epidote-quartz vein samples (06HLT7 and 06HLT8) also show higher ε^{205}Tl of +1.1 (Table 2) compared to the distal eclogite. Three kyanite-epidote-quartz vein

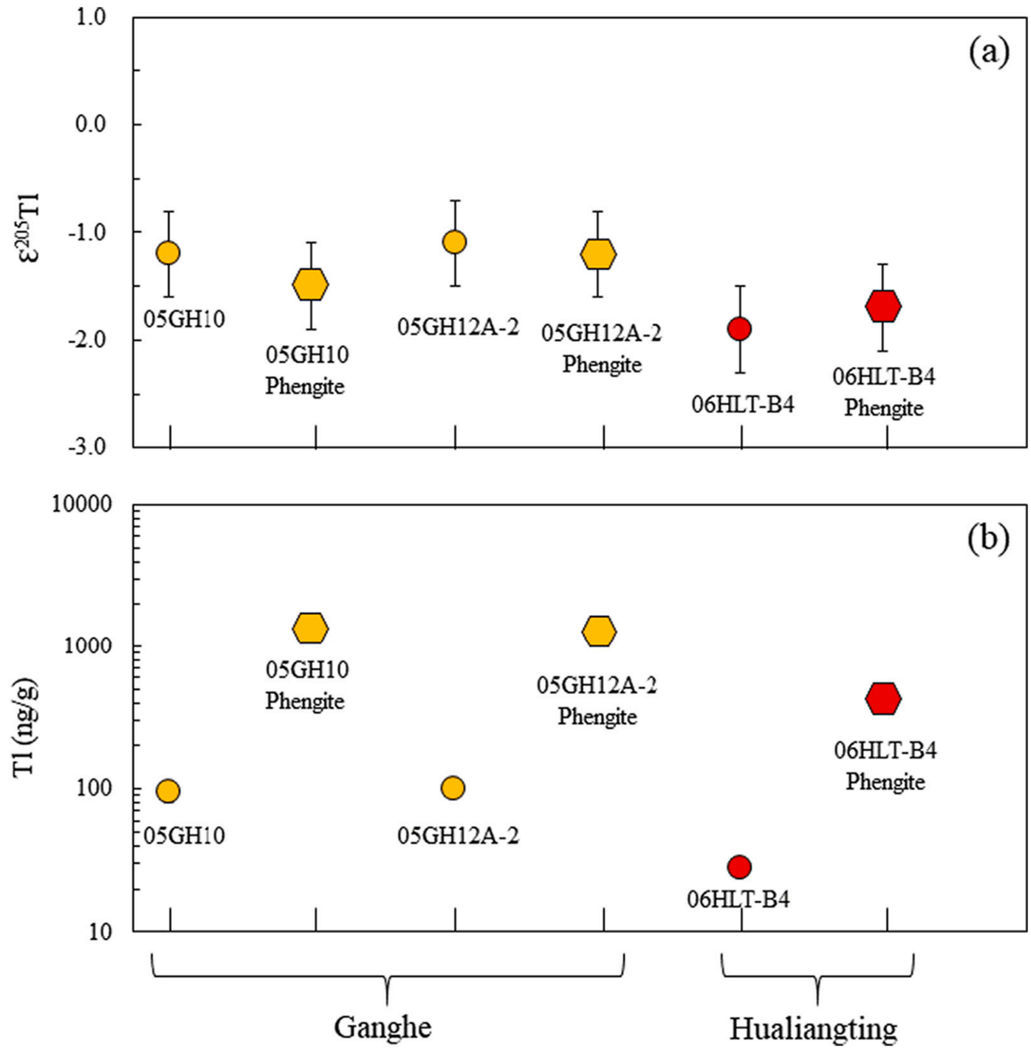

Fig. 6. Thallium concentration and thallium isotope characteristics of phengites and their host eclogites from Ganghe and Hualiangting.

samples (06HLT4, 06HLT5 and 06HLT6) from the interior of the vein systems exhibit $\varepsilon^{205}Tl = -2.2$, -2.3 and -2.5 respectively (Table 2), similar to the eclogite. Thallium concentrations of the eclogites near the vein range from 5.64 to 35.6 ng/g (Table 2). The distal eclogite displays Tl concentration of 3.39 ng/g (Table 2). All three types of veins have lower Tl abundances from 0.54 to 1.98 ng/g than their host eclogites (Table 2).

5. Discussion

5.1. Effect of retrograde metamorphism on thallium isotope fractionation

Although the eclogites and veins in this study were carefully selected to avoid retrogression features and alteration that could result in Tl addition and/or loss (Guo et al., 2012; Guo et al., 2015a), it is still necessary to assess the effect of retrograde metamorphism on their Tl isotope compositions before further discussion. Oceanic eclogites without superimposed effects of metasomatism by externally-derived fluids during subduction-related metamorphism have been shown to inherit the Tl isotope compositions of their protoliths (Shu et al., 2019), suggesting retrogression would not be expected to cause notable Tl isotope effects either. This inference can be further tested by comparing Tl isotope values between a pair of pristine sample and minimally retrogressed sample that have similar mineralogies (e.g. vein 05GH12A versus vein 05GH12). Minimally retrogressed sample displays identical Tl isotope composition compared to fresh sample. Therefore, the effect of retrograde metamorphism on whole-rock Tl isotope compositions appears to be limited for the samples studied here.

5.2. Phengite controls thallium budget in the subducted slab

Phengite contains significant concentrations of alkali elements such as K, Rb, Cs and Ba (Zack et al., 2001; Bebout, 2007; Guo et al., 2012; Guo et al., 2015a; Gu et al., 2021). The chemical behavior of Tl is considered to group with the heavy alkali metals K, Rb and Cs, due to their similar ionic radii and charge (Shaw, 1952; Shannon, 1976; Heinrichs et al., 1980). Therefore, previous studies of arc lavas suggest that when present, phengite exerts a strong control on Tl in the subducted slab (Prytulak et al., 2013; Nielsen et al., 2016; Nielsen et al., 2017). A recent study of subducted oceanic crust supports this inference because phengite-bearing metamorphic rocks have much higher Tl abundances than phengite-free samples (Shu et al., 2019). In situ mineralogical study also reveals that phengite is main host of Tl in metapelite and metacarbonate rocks, especially during prograde metamorphism (Rader et al., 2021). The vein samples in Ganghe and Hualiangting analyzed in this study generally contain less phengite than their host phengite-bearing eclogites, and lower Tl concentrations (Figs. 3 and 4, Table 1). Moreover, thallium concentrations in the host eclogites positively correlate with K, Rb, Cs and Ba concentrations, all controlled by the abundance of phengite (Fig. 5). No correlation is observed between Tl and Cu concentrations (Fig. 5), which suggests that sulfide is not a significant host of Tl in the eclogite-vein systems. Recent study by Shu et al. (2019) presented Tl concentration and isotope data for samples of subducted oceanic crust and found that Tl concentrations in most samples follow strong linear relationships with K, Rb, Cs and Ba. Our observations in the present study agree with previous findings that phengite strongly controls Tl concentrations in the subducted slab (Shu et al., 2019). In addition, phengite-free metamorphic rocks with low Tl contents display Tl isotope compositions largely overlapping with that of phengite-bearing samples from the same locations, which implies that the stabilization or breakdown of phengite does not induce significant Tl isotope fractionation in subducted slabs (Shu et al., 2019). This interpretation is supported by our analyses of phengite mineral separates from eclogite 06HLT-B4 near the Hualiangting veins and eclogite 05GH12A-2 near the Ganghe vein, as well as eclogite 05GH10 far from the Ganghe vein. These mineral separates reveal that Tl concentrations in phengites are an order of magnitude higher than their host eclogites (Fig. 6), which confirms phengite as the dominant host of Tl. Based on Tl concentrations and estimated modal abundances of phengite in the Tables 1 and 2, samples 05GH12A-2 and 06HLT-B4 were calculated to contain Tl concentrations of ~127 and 22 ng/g respectively, which are similar to the bulk Tl concentrations of 101 and 28.4 ng/g (Table 2). Sample 05GH10 has ~40 ng/g Tl calculated from phengite abundances and Tl concentrations in the phengite separate but displays bulk Tl contents of 95.5 ng/g (Table 2). It is notable that the sample 05GH10 with the biggest mismatch also has the lowest modal abundance of phengite (3% in Table 1) among these three samples and thus the modal abundance of phengite in 05GH10 is the most uncertain. The modal abundances were estimated using point counting in thin sections (Guo et al., 2012; Guo et al., 2015a), which can be inaccurate if the thin sections and the splits of sample powders have different modal mineralogy. In addition, a recent study reveals that phengite also appears to control Ba isotope systematics in these samples, as phengite incorporates >95% of the bulk Ba budget in the host eclogites and also displays Ba isotope composition identical to the host eclogites (Gu et al., 2021).

5.3. Thallium isotope compositions of vein-forming fluids in the subducted slab

The Ganghe omphacite-epidote vein (phengite-free) displays similar Tl isotope value to their host eclogites (phengite-bearing) (Fig. 3). Thjs result is consistent with previous inferences based on whole-rock and epidote in situ Sr isotope analyses that the fluid responsible for the HP veins was derived from the host eclogite itself rather than from external gneisses in a geochemically closed system (Guo et al., 2014). Thallium is known to be fluid-mobile (Shaw, 1952; Shannon, 1976; Heinrichs et al., 1980; Nielsen et al., 2014; Nielsen et al., 2017) and, consequently, Tl isotope fractionation could in theory occur when Tl partitions between phengite and the fluid phase. However, despite the fact that the Ganghe eclogites and veins display a large range in Tl concentrations varying by a factor of 50 over ~20 cm outcrop (Fig. 3b), the Tl isotope compositions of all these rocks are the same within error. Therefore, substantial Tl redistribution has not occurred after vein formation, and Tl isotope fractionation did not occur during fluid-release. Based on these observations, we infer that Tl isotope fractionation also did not occur during fluid production in the Hualiangting rocks. These conclusions are consistent with a previous study where eclogites from the Cabo Ortegal and Raspas Complexes preserved the Tl isotope compositions of their protoliths during eclogitization and metasomatism by fluids derived internally from dehydration of the protolith itself (Shu et al., 2019).

Like the Ganghe vein samples, the Hualiangting veins exhibit very low Tl concentrations, suggesting that the fluids that produced these veins were also formed by lawsonite breakdown in the presence of residual phengite. In contrast to homogeneous Tl isotope signatures in Ganghe samples, the multiple veins at Hualiangting exhibit ε^{205}Tl values from −2.5 to +1.6 (Fig. 4). The omphacite-epidote and epidote-quartz veins display ε^{205}Tl = −0.9 to +1.6 different from the eclogite far from the veins (ε^{205}Tl = −2.8) and eclogites near the veins (ε^{205}Tl ~ −1.9), while the innermost kyanite-epidote-quartz vein samples show ε^{205}Tl = −2.2 to −2.5 within error of the host eclogites (Fig. 4). If lawsonite breakdown in the presence of phengite does not induce Tl isotope fractionation, then the variable Tl isotope compositions of Hualiangting veins could reflect isotope fractionation during precipitation of minor minerals in the veins, as omphacite/epidote precipitation does not appear to fractionate Tl isotopes in the Ganghe samples. The omphacite-epidote and epidote-quartz veins do not contain phengite and display very low Tl concentrations, which render it difficult to infer the primary host mineral of Tl in the veins. The omphacite-epidote, epidote-quartz and kyanite-epidote-quartz veins all have invariant initial Sr isotope compositions that are identical to the host eclogite, suggesting that they precipitated successively from a host eclogite-derived fluid (Guo et al., 2015a). In this case, Tl isotope fractionation and concomitant fluid evolution may have produced the observed Tl isotope data due to isotopically heavy Tl being removed from the fluid into the veins, thus, producing successively lighter fluid compositions. It is, however, difficult to explain why we observe these isotope fractionation patterns at Hualiangting and not Ganghe, where the mineralogy of some of the veins overlap.

Alternatively, Tl isotope variability could reflect Tl isotope variations of the source rocks (currently unsampled by our subset of eclogites). At first this interpretation may seem at odds with the invariant Sr isotope compositions in the eclogite and veins (Guo et al., 2015a) that suggests a single, homogeneous source rock for the fluids. However, lawsonite, which is the primary source of the fluids (Guo et al., 2015a), is characterized by high Sr abundances (Martin et al., 2014; Whitney et al., 2020), whereas it is not likely to be a major host of Tl. For this reason, any minor contribution of fluid from other lithologies would be unlikely to modify the Sr isotope composition of the fluid whereas Tl isotopes could readily be affected. For example, meta-sediments are known to exhibit heavy (positive) Tl isotope compositions (Shu et al., 2019), and small contributions from a sediment-derived fluid would, thus, be readily apparent in the Tl isotope system, but not in Sr isotopes. The decoupling of Sr and Tl isotopes was also observed in several studies of OIBs (Blusztajn et al., 2018; Brett et al., 2021), suggesting that processes in which Sr and Tl are affected differentially are not uncommon. Low Cs/Tl observed in the omphacite-epidote vein in the Hualiangting samples is consistent with the presence of pelagic sediment components, which typically display Cs/Tl < 10 (Nielsen et al., 2016; Nielsen et al., 2017; Shu et al., 2017), and consistent with heavy Tl isotope values in these samples. In addition, the variable in situ Sr isotope values of epidote in amphibolites collected from the margin of the metamorphic block clearly indicate the involvement of external fluid (Guo et al., 2016; Guo et al., 2017). In addition, Ba isotope study in the Hualiangting veins also indicates existence of external fluids derived from the country rocks (Gu et al., 2021). The temporal evolution of the Tl isotope composition of the veins from heavy values in the early veins toward host eclogite-like values in the latest vein could also suggest that the minor sedimentary source material had been exhausted during the early stages of fluid percolation.

5.4. Implication for arc magmatism

Recent studies have argued that subducted materials, which have high Tl concentrations and distinctive Tl isotope signatures, play a dominant role in affecting Tl isotope compositions of arc and back-arc magmatism (Nielsen et al., 2016; Nielsen et al., 2017; Shu et al., 2017). Furthermore, it has been suggested that slab-derived fluids or melts with phengite in the residue might produce high Cs/Tl ratios in arc lavas because the ionic radius of Tl is most similar to that of Rb (Shannon, 1976), and Cs is less compatible than Rb in phengite (Melzer and Wunder, 2000; Busigny et al., 2003; Bebout et al., 2004; Bebout, 2007; Hermann and Rubatto, 2009). The Cs/Tl ratios observed in the Dabie

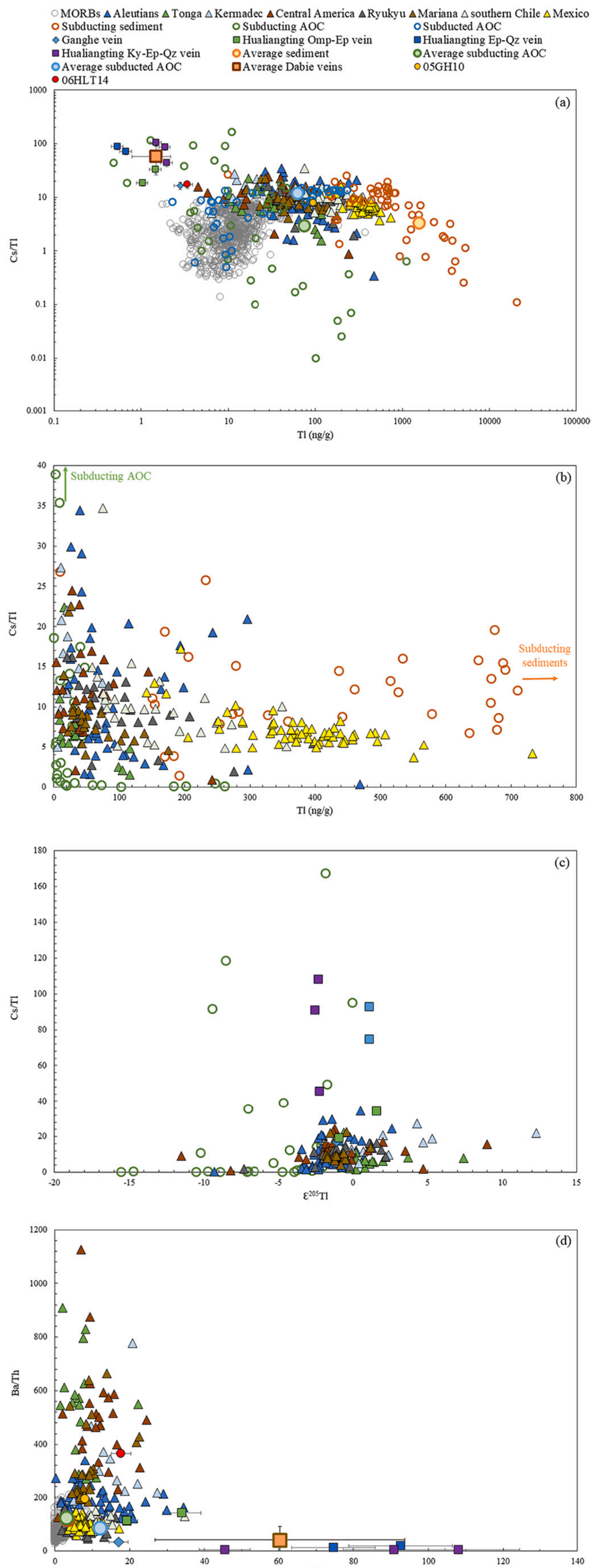

(caption on next column)

Fig. 7. Cs/Tl vs (a) and (b) Tl concentrations, (c) Tl isotope compositions and (d) Ba/Th for Ganghe and Hualiangting veins and arc lavas. Global MORBs, subducting altered oceanic crust (AOC) and sediments as well as subducted AOC (oceanic eclogite) samples are shown for comparison. Data sources: Aleutians (Plank, 2005; Yogodzinski et al., 2015; Nielsen et al., 2016); Tonga-Kermadec (Ewart et al., 1998; Nielsen et al., 2017); Central America (Carr et al., 2014; Nielsen et al., 2017); Ryukyu (Shu et al., 2017); Mariana (Wade et al., 2005; Prytulak et al., 2013; Prytulak et al., 2017); southern Chile (Cox et al., 2019); Mexico (Mangler et al., 2019); MORBs (Jenner and O'Neill, 2012; Nielsen et al., 2014; Yang et al., 2018); subducted AOC (Shu et al., 2019); subducting AOC and sediments outboard of global arcs (Nielsen et al., 2006c; Prytulak et al., 2013; Coggon et al., 2014; Nielsen et al., 2016; Nielsen et al., 2017; Shu et al., 2017). Only distal eclogites that were not affected by vein-forming fluids from Ganghe and Hualiangting are shown in the figure.

veins support this inference as the veins preserve Cs/Tl ratios that are on average higher (60 ± 33, 1sd, $n = 8$) than Cs/Tl ratios in the distal host eclogites (12.9 ± 4.8, 1sd, $n = 2$) unaffected by fluid-rock interaction (Fig. 3c, 4c and 7). Phengite incorporates >90% of the budgets of Ba, Cs and Rb in eclogite whole rocks (Zack et al., 2001; Bebout, 2007), whereas Th is controlled by accessory phases like monazite and epidote-group minerals (Zack et al., 2002; Spandler et al., 2003; Hermann and Rubatto, 2009). Therefore, residual phengite in the source of fluids will result in high Ba/Th ratios in the eclogitic residue and low Ba/Th values in arc lavas. The low Ba/Th ratios observed in the Dabie veins also support this inference (Fig. 7d). However, when aqueous fluids are produced by the breakdown of phengite, Ba will be preferentially transported into the source region of arc lavas resulting in high Ba/Th in the melt. Since both Cs and Tl are primarily hosted by phengite, destabilization of phengite will effectively transfer significant Cs and Tl to the melt resulting in similar Cs/Tl values compared to phengite-rich eclogites (Shu et al., 2019). Global arc lavas from the Aleutians, Marianas, Central America and Tonga-Kermadec arcs display hyperbolic relationships between Cs/Tl and Ba/Th ratios, which was interpreted to reflect the stability of phengite in the slab (Nielsen et al., 2017). Therefore, elemental systematics and absolute Tl concentrations in eclogite-hosted veins support the formation of fluids with high Cs/Tl ratios in the presence of residual phengite, as hypothesized in several previous studies (Prytulak et al., 2013; Nielsen et al., 2016; Nielsen et al., 2017; Shu et al., 2017). Results from this study predict that arc lavas where at least part of the fluids are released from the breakdown of lawsonite in the presence of residual phengite would be associated with high Cs/Tl and low Ba/Th ratios (Fig. 7d).

Subducting sediments outboard the Aleutians, Ryukyu, Marianas and Tonga-Kermadec arcs display Cs/Tl ranging from 0.1 to 26.8 (Prytulak et al., 2013; Nielsen et al., 2016; Nielsen et al., 2017; Shu et al., 2017), with average values of 3.4 ($n = 53$; Table S2), of which 2 samples (Cs/Tl = 25.8 and 26.8; Table S2) have Cs/Tl > 20. Subducting sediments, thus, have a smaller range of Cs/Tl (0.1 to 26.8) than global arc lavas (Cs/Tl = 0.3 to 34.7) (Fig. 7). Subducting altered oceanic crust (AOC) samples outboard of global arcs exhibit more variable Cs/Tl, ranging from 0.01 to 167 (Nielsen et al., 2006c; Prytulak et al., 2013; Coggon et al., 2014; Shu et al., 2017). However, the vast majority of these exhibit low values such that the average Cs/Tl = 3.0 ($n = 36$; Table S2). In addition, AOC samples are usually characterized by light Tl isotope compositions with ε^{205}Tl < −2, but the arc lavas with Cs/Tl > 20 all show ε^{205}Tl > −2 (Fig. 7c). Therefore, there is no evidence to suggest that AOC samples play an important role in the generation of the arc lavas with high Cs/Tl. Lastly, all subducted AOC (oceanic eclogite) samples from different locations globally show Cs/Tl < 16 (Shu et al., 2019), with a much tighter distribution of values resulting in an average Cs/Tl = 12.1 ($n = 38$; Table S2), similar to the distal eclogites in this study (Fig. 7a). It indicates that AOC samples are likely modified to a relatively narrow range of Cs/Tl by subduction processes before or during their contribution to arc magmas. It is also worth noting that a few subducting AOC samples with high Cs/Tl are characterized by low Tl concentrations compared to other samples with Cs/Tl < 15 (Fig. 7a), which prevents these samples as primary medium of Tl cycling in subduction zones. All together the compiled literature data for sediments and AOC demonstrate that high Cs/Tl ratios in arc lavas corrected for Tl degassing (Nielsen et al., 2021) are unlikely to be influenced by spuriously high Cs/Tl in the subducted slab, as all subducting and subducted slab components exhibit average Cs/Tl < 13 (Table S2). Here, we propose that Cs/Tl values >15 in arc magmas can be confidently attributed to fractionation during subduction rather than source variations.

Most arc lavas with higher Cs/Tl ratios (>15) than subducted AOC and sediments, are characterized by low Tl concentrations (Fig. 7), which is best attributed to the effect of the fluids derived from a source with residual phengite present. Such systematics have been observed in arc lavas from the Aleutians, Tonga-Kermadec, Central America and Mariana arcs (Nielsen et al., 2017). High Cs/Tl has been reported for a relatively small proportion of arc lavas, but lavas with high Cs/Tl are observed in arcs globally. Although lower Cs/Tl in arc magmas would not preclude the presence of phengite at depth, arc magmas that display high Cs/Tl ratios (>15) and low Ba/Th ratios should provide the most definite record of the presence of residual phengite at subarc depths.

6. Conclusions

This study presents high-precision Tl isotope data for two suites of HP metamorphic veins and host UHP eclogites at Ganghe and Hualiangting areas in the Dabie terrane. When present, phengite is the dominant host for Tl in eclogite. In addition, eclogite dehydration did not lead to Tl isotope fractionation between the source eclogite and the fluids. Phengite had to be present in the eclogitic residue during lawsonite breakdown, as supported by the low Tl abundances of the veins formed during fluid release. The Ganghe metamorphic vein was formed by fluid derived internally from dehydration of lawsonite in the host eclogites and preserved the Tl isotope composition of the original eclogite. The Hualiangting multiple stage veins display variable Tl isotope compositions. It most likely indicates that some of the fluids were contaminated by a minor sediment component which exhibits heavy Tl isotope characteristics of $\varepsilon^{205}Tl \sim +2$. The Cs/Tl ratios in the Ganghe and Hualiangting veins are on average higher than those of the host eclogites unaffected by fluid-rock interaction. We argue that slab-derived fluids produced in the presence of phengite can carry high Cs/Tl ratios, and could be traced particularly well in the chemistry of some arc lavas.

Declaration of Competing Interest

None.

Acknowledgments

We would like to thank Alex Brett and an anonymous reviewer for insightful comments that helped improve this manuscript and Catherine Chauvel for her editorial handling. This study was financially supported by grants from the National Natural Science Foundation of China (No. 41903008) and the China Postdoctoral Science Foundation (2019M660153) to YS, NSF grants EAR-1839128 to VLR and EAR-1829546 to SGN, and National Natural Science Foundation of China (No. 41922013) to SG. We gratefully thank Maureen Auro, Tristan Horner and the rest of the NIRVANA group at WHOI for keeping clean labs and the WHOI plasma facility functioning at all times. We also thank Jian Huang for providing several samples.

Declaration of Competing Interest

The authors declare that they have no conflict of interest.

Appendix A. Supplementary data

Supplementary data to this article can be found online at https://doi.org/10.1016/j.chemgeo.2022.120843.

References

Bebout, G.E., 2007. Metamorphic chemical geodynamics of subduction zones. Earth Planet. Sci. Lett. 260 (3–4), 373–393.

Bebout, G., Agard, P., King, R., Nakamura, E., 2004. Record of Forearc Devolatilization in the Schistes Lustrés HP–UHP Metasedimentary Unit Western Alps, Proc. Eleventh Water–Rock Symposium, Saratoga Springs.

Blusztajn, J., et al., 2018. Thallium isotope systematics in volcanic rocks from St. Helena – Constraints on the origin of the HIMU reservoir. Chem. Geol. 476, 292–301.

Brett, E.K.A., et al., 2021. Thallium elemental and isotopic systematics in ocean island lavas. Geochim. Cosmochim. Acta 301, 187–210.

Busigny, V., Cartigny, P., Philippot, P., Ader, M., Javoy, M., 2003. Massive recycling of nitrogen and other fluid-mobile elements (K, Rb, Cs, H) in a cold slab environment: evidence from HP to UHP oceanic metasediments of the Schistes Lustrés nappe (western Alps, Europe). Earth Planet. Sci. Lett. 215 (1–2), 27–42.

Carr, M.J., Feigenson, M.D., Bolge, L.L., Walker, J.A., Gazel, E., 2014. RU _ CAG eochem, a database and sample repository for central American volcanic rocks at Rutgers University. Geoscience Data Journal 1 (1), 43–48.

Castelli, D., Rolfo, F., Compagnoni, R., Xu, S., 1998. Metamorphic veins with kyanite, zoisite and quartz in the Zhu-Jia-Chong eclogite, Dabie Shan, China. Island Arc 7 (1–2), 159–173.

Coggon, R.M., et al., 2014. Controls on thallium uptake during hydrothermal alteration of the upper ocean crust. Geochim. Cosmochim. Acta 144, 25–42.

Cox, D., Watt, S.F.L., Jenner, F.E., Hastie, A.R., Hammond, S.J., 2019. Chalcophile element processing beneath a continental arc stratovolcano. Earth Planet. Sci. Lett. 522, 1–11.

Ewart, A., Collerson, K., Regelous, M., Wendt, J., Niu, Y., 1998. Geochemical evolution within the Tonga–Kermadec–Lau arc–back-arc systems: the role of varying mantle wedge composition in space and time. J. Petrol. 39 (3), 331–368.

Franz, L., et al., 2001. Eclogite-facies quartz veins within metabasites of the Dabie Shan (eastern China): pressure-temperature-time-deformation path, composition of the fluid phase and fluid flow during exhumation of high-pressure rocks. Contrib. Mineral. Petrol. 141 (3), 322–346.

Gao, J., Klemd, R., 2001. Primary fluids entrapped at blueschist to eclogite transition: evidence from the Tianshan meta-subduction complex in northwestern China. Contrib. Mineral. Petrol. 142 (1), 1–14.

Gao, J., John, T., Klemd, R., Xiong, X., 2007. Mobilization of Ti–Nb–Ta during subduction: evidence from rutile-bearing dehydration segregations and veins hosted in eclogite, Tianshan, NW China. Geochimica et Cosmochimica Acta 71 (20), 4974–4996.

Gu, X.-F., Guo, S., Yu, H., Xu, J., Huang, F., 2021. Behavior of barium isotopes during high-pressure metamorphism and fluid evolution. Earth Planet. Sci. Lett. 575, 117176.

Guo, S., et al., 2012. Fluid–rock interaction and element mobilization in UHP metabasalt: Constraints from an omphacite–epidote vein and host eclogites in the Dabie orogen. Lithos 136-139, 145–167.

Guo, S., et al., 2014. In situ Sr isotopic analyses of epidote: tracing the sources of multi-stage fluids in ultrahigh-pressure eclogite (Ganghe, Dabie terrane). Contrib. Mineral. Petrol. 167, 975.

Guo, S., et al., 2015a. Formation of multiple high-pressure veins in ultrahigh-pressure eclogite (Hualiangting, Dabie terrane, China): Fluid source, element transfer, and closed-system metamorphic veining. Chem. Geol. 417, 238–260.

Guo, S., et al., 2015b. Metamorphic P-T trajectory and multi-stage fluid events of vein-bearing UHP eclogites from the Dabie terrane: insights from compositional zonations of key minerals. Int. Geol. Rev. 57 (9–10), 1077–1102.

Guo, S., et al., 2016. Grain-scale Sr isotope heterogeneity in amphibolite (retrograded UHP eclogite, Dabie terrane): Implications for the origin and flow behavior of retrograde fluids during slab exhumation. Lithos 266-267, 383–405.

Guo, S., et al., 2017. Unusual replacement of Fe-Ti oxides by rutile during retrogression in amphibolite-hosted veins (Dabie UHP terrane): a mineralogical record of fluid-induced oxidation processes in exhumed UHP slabs. Am. Mineral. 102 (11), 2268–2283.

Harvey, J., et al., 2014. 11B-rich fluids in subduction zones: the role of antigorite dehydration in subducting slabs and boron isotope heterogeneity in the mantle. Chem. Geol. 376, 20–30.

Heinrichs, H., Schulz-Dobrick, B., Wedepohl, K., 1980. Terrestrial geochemistry of Cd, Bi, Tl, Pb, Zn and Rb. Geochim. Cosmochim. Acta 44 (10), 1519–1533.

Hermann, J., Rubatto, D., 2009. Accessory phase control on the trace element signature of sediment melts in subduction zones. Chem. Geol. 265 (3–4), 512–526.

Huang, J., Guo, S., Jin, Q.-Z., Huang, F., 2020. Iron and magnesium isotopic compositions of subduction-zone fluids and implications for arc volcanism. Geochim. Cosmochim. Acta 278, 376–391.

Jenner, F.E., O'Neill, H.S.C., 2012. Analysis of 60 elements in 616 ocean floor basaltic glasses. Geochem. Geophys. Geosyst. 13 (2), n/a–n/a.

Kendrick, M.A., et al., 2014. Subduction-related halogens (Cl, Br and I) and H2O in magmatic glasses from Southwest Pacific Backarc Basins. Earth Planet. Sci. Lett. 400, 165–176.

Keppler, H., 2017. Fluids and trace element transport in subduction zones. Am. Mineral. 102 (1), 5–20.

Kessel, R., Schmidt, M.W., Ulmer, P., Pettke, T., 2005. Trace element signature of subduction-zone fluids, melts and supercritical liquids at 120–180 km depth. Nature 437 (7059), 724–727.

Li, S., 1993. Collision of the North China and Yangtze blocks and formation of coesite-bearing eclogites; timing and processes. Chem. Geol. 112, 243–350.
Li, S., et al., 1993. Collision of the North China and Yangtse Blocks and formation of coesite-bearing eclogites: timing and processes. Chem. Geol. 109 (1–4), 89–111.
Li, Y., Yu, H., Gu, X., Guo, S., Huang, F., 2020. Silicon isotopic fractionation during metamorphic fluid activities: constraints from eclogites and ultrahigh-pressure veins in the Dabie orogen, China. Chemical Geology 540, 119550.
Liu, Y.C., Li, S.G., Gu, X.F., Xu, S.T., Chen, G.B., 2007. Ultrahigh-pressure eclogite transformed from mafic granulite in the Dabie orogen, east-Central China. J. Metamorph. Geol. 25 (9), 975–989.
Mangler, M., Prytulak, J., Gisbert, G., Delgado-Granados, H., Petrone, C.M., 2019. Interplinian Effusive Activity at Popocatépetl Volcano, Mexico: New insights into evolution and dynamics of the plumbing system.
Martin, L.A.J., et al., 2014. Lawsonite geochemistry and stability - implication for trace element and water cycles in subduction zones. J. Metamorph. Geol. 32 (5), 455–478.
Massonne, H.-J., 2012. Formation of amphibole and clinozoisite–epidote in eclogite owing to fluid infiltration during exhumation in a subduction channel. J. Petrol. 53 (10), 1969–1998.
Melzer, S., Wunder, B., 2000. Island-arc basalt alkali ratios: Constraints from phengite-fluid partitioning experiments. Geology 28 (7), 583–586.
Nielsen, S.G., Rehkämper, M., Baker, J., Halliday, A.N., 2004. The precise and accurate determination of thallium isotope compositions and concentrations for water samples by MC-ICPMS. Chem. Geol. 204 (1–2), 109–124.
Nielsen, S.G., Rehkämper, M., Halliday, A.N., 2006a. Large thallium isotopic variations in iron meteorites and evidence for lead-205 in the early solar system. Geochim. Cosmochim. Acta 70 (10), 2643–2657.
Nielsen, S.G., Rehkamper, M., Norman, M.D., Halliday, A.N., Harrison, D., 2006b. Thallium isotopic evidence for ferromanganese sediments in the mantle source of Hawaiian basalts. Nature 439 (7074), 314–317.
Nielsen, S.G., et al., 2006c. Hydrothermal fluid fluxes calculated from the isotopic mass balance of thallium in the ocean crust. Earth Planet. Sci. Lett. 251 (1–2), 120–133.
Nielsen, S.G., et al., 2007. Thallium isotopes in Iceland and Azores lavas — Implications for the role of altered crust and mantle geochemistry. Earth Planet. Sci. Lett. 264 (1–2), 332–345.
Nielsen, S.G., et al., 2013. Towards an understanding of thallium isotope fractionation during adsorption to manganese oxides. Geochim. Cosmochim. Acta 117, 252–265.
Nielsen, S.G., Shimizu, N., Lee, C.T.A., Behn, M.D., 2014. Chalcophile behavior of thallium during MORB melting and implications for the sulfur content of the mantle. Geochem. Geophys. Geosyst. 15 (12), 4905–4919.
Nielsen, S.G., Klein, F., Kading, T., Blusztajn, J., Wickham, K., 2015. Thallium as a tracer of fluid–rock interaction in the shallow Mariana forearc. Earth Planet. Sci. Lett. 430, 416–426.
Nielsen, S.G., et al., 2016. Tracking along-arc sediment inputs to the Aleutian arc using thallium isotopes. Geochim. Cosmochim. Acta 181, 217–237.
Nielsen, S.G., et al., 2017. Thallium isotopes as tracers of recycled materials in subduction zones: Review and new data for lavas from Tonga-Kermadec and Central America. J. Volcanol. Geotherm. Res. 339, 23–40.
Nielsen, S.G., et al., 2021. Thallium Isotope Fractionation during Magma Degassing: evidence from experiments and Kamchatka Arc Lavas. Geochem. Geophys. Geosyst. 22, e2020GC009608.
Owens, J.D., Nielsen, S.G., Horner, T.J., Ostrander, C.M., Peterson, L.C., 2017. Thallium-isotopic compositions of euxinic sediments as a proxy for global manganese-oxide burial. Geochim. Cosmochim. Acta 213, 291–307.
Peacock, S.A., 1990. Fluid processes in subduction zones. Science 248 (4953), 329–337.
Plank, T., 2005. Constraints from Thorium/Lanthanum on Sediment Recycling at Subduction zones and the Evolution of the Continents. J. Petrol. 46 (5), 921–944.
Prytulak, J., Nielsen, S.G., Plank, T., Barker, M., Elliott, T., 2013. Assessing the utility of thallium and thallium isotopes for tracing subduction zone inputs to the Mariana arc. Chem. Geol. 345, 139–149.
Prytulak, J., et al., 2017. Thallium elemental behavior and stable isotope fractionation during magmatic processes. Chem. Geol. 448, 71–83.
Rader, S.T., et al., 2021. Thallium behavior during high-pressure metamorphism in the Western Alps, Europe. Chemical Geology 579, 120349.
Rehkämper, M., Halliday, A.N., 1999. The precise measurement of Tl isotopic compositions by MC-ICPMS: application to the analysis of geological materials and meteorites. Geochim. Cosmochim. Acta 63 (6), 935–944.
Rehkämper, M., et al., 2002. Thallium isotope variations in seawater and hydrogenetic, diagenetic, and hydrothermal ferromanganese deposits. Earth Planet. Sci. Lett. 197 (1–2), 65–81.
Rehkämper, M., Frank, M., Hein, J.R., Halliday, A., 2004. Cenozoic marine geochemistry of thallium deduced from isotopic studies of ferromanganese crusts and pelagic sediments. Earth Planet. Sci. Lett. 219 (1–2), 77–91.
Scambelluri, M., Pettke, T., Cannaò, E., 2015. Fluid-related inclusions in Alpine high-pressure peridotite reveal trace element recycling during subduction-zone dehydration of serpentinized mantle (Cima di Gagnone, Swiss Alps). Earth Planet. Sci. Lett. 429, 45–59.
Shannon, R.D., 1976. Revised effective ionic radii and systematic studies of interatomic distances in halides and chalcogenides. Acta Crystallogr. Sect. A: Cryst. Phys., Diffr., Theor. Gen. Crystallogr. 32 (5), 751–767.
Shaw, D.M., 1952. The geochemistry of thallium. Geochim. Cosmochim. Acta 2 (2), 118–154.
Shu, Y., et al., 2017. Tracing subducted sediment inputs to the Ryukyu arc-Okinawa Trough system: evidence from thallium isotopes. Geochim. Cosmochim. Acta 217, 462–491.
Shu, Y., et al., 2019. Closing the loop: Subducted eclogites match thallium isotope compositions of ocean island basalts. Geochim. Cosmochim. Acta 250, 130–148.
Spandler, C., Hermann, J., 2006. High-pressure veins in eclogite from New Caledonia and their significance for fluid migration in subduction zones. Lithos 89 (1–2), 135.
Spandler, C., Hermann, J.R., Arculus, R., Mavrogenes, J., 2003. Redistribution of trace elements during prograde metamorphism from lawsonite blueschist to eclogite facies; implications for deep subduction-zone processes. Contrib. Mineral. Petrol. 146 (2), 205–222.
Ulmer, P., Trommsdorff, V., 1995. Serpentine stability to mantle depths and subduction-related magmatism. Science 268 (5212), 858–861.
Villalobos-Orchard, J., et al., 2020. Molybdenum isotope ratios in Izu arc basalts: the control of subduction zone fluids on compositional variations in arc volcanic systems. Geochim. Cosmochim. Acta 288, 68–82.
Wade, J.A., et al., 2005. The May 2003 eruption of Anatahan volcano, Mariana Islands: Geochemical evolution of a silicic island-arc volcano. J. Volcanol. Geotherm. Res. 146 (1–3), 139–170.
Whitney, D.L., et al., 2020. Lawsonite composition and zoning as tracers of subduction processes: a global review. Lithos 370-371, 105636.
Williamson, N.M.B., Weis, D., Prytulak, J., 2021. Thallium isotopic compositions in hawaiian lavas: evidence for recycled materials on the kea side of the Hawaiian Mantle Plume. Geochem. Geophys. Geosyst. 22, e2021GC009765.
Xu, S., et al., 1992. Diamond from the Dabie Shan metamorphic rocks and its implication for tectonic setting. Science 256 (5053), 80–82.
Yang, S., Humayun, M., Salters, V.J., 2018. Elemental systematics in MORB glasses from the Mid-Atlantic Ridge. Geochem. Geophys. Geosyst. 19 (11), 4236–4259.
Yogodzinski, G.M., et al., 2015. The Role of Subducted Basalt in the source of Island Arc Magmas: evidence from Seafloor Lavas of the Western Aleutians. J. Petrol. 56 (3), 441–492.
Zack, T., Rivers, T., Foley, S., 2001. Cs–Rb–Ba systematics in phengite and amphibole: an assessment of fluid mobility at 2.0 GPa in eclogites from Trescolmen, Central Alps. Contrib. Mineral. Petrol. 140 (6), 651–669.
Zack, T., Foley, S., Rivers, T., 2002. Equilibrium and disequilibrium trace element partitioning in hydrous eclogites (Trescolmen, Central Alps). J. Petrol. 43 (10), 1947–1974.
Zhang, R., Liou, J., Tsai, C., 1996. Petrogenesis of a high-temperature metamorphic terrane: a new tectonic interpretation for the north Dabieshan, Central China. J. Metamorph. Geol. 14 (3), 319–333.
Zhang, R., Liou, J., Ernst, W., 2009. The Dabie–Sulu continental collision zone: a comprehensive review. Gondwana Res. 16 (1), 1–26.
Zhao, Y., Zheng, J.-P., Xiong, Q., Zhang, H., 2018. Destruction of the North China Craton triggered by the Triassic Yangtze continental subduction/collision: a review. J. Asian Earth Sci. 164, 72–82.
Zheng, Y.-F., Fu, B., Gong, B., Li, L., 2003. Stable isotope geochemistry of ultrahigh pressure metamorphic rocks from the Dabie–Sulu orogen in China: implications for geodynamics and fluid regime. Earth Sci. Rev. 62 (1–2), 105–161.
Zheng, J., Griffin, W., O'Reilly, S.Y., Zhang, M., Pearson, N., 2006a. Zircons in mantle xenoliths record the Triassic Yangtze–North China continental collision. Earth Planet. Sci. Lett. 247 (1–2), 130–142.
Zheng, Y.-F., et al., 2006b. Zircon U–Pb age, Hf and O isotope constraints on protolith origin of ultrahigh-pressure eclogite and gneiss in the Dabie orogen. Chem. Geol. 231 (1–2), 135–158.
Zheng, Y.-F., Chen, R.-X., Zhao, Z.-F., 2009. Chemical geodynamics of continental subduction-zone metamorphism: Insights from studies of the Chinese Continental Scientific Drilling (CCSD) core samples. Tectonophysics 475 (2), 327–358.
Zhu, J., Zhang, L., Tao, R., Fei, Y., 2020. The formation of graphite-rich eclogite vein in SW Tianshan (China) and its implication for deep carbon cycling in subduction zone. Chem. Geol. 533, 119430.